

Toward scatter-free phosphors in white phosphor-converted light-emitting diodes

Hoo Keun Park, Ji Hye Oh, and Young Rag Do*

Department of Chemistry, Kookmin University, Seoul 136-702, South Korea

*yrdo@kookmin.ac.kr

Abstract: Scatter-free phosphors promise to suppress the scattering loss of conventional micro-size powder phosphors in white phosphor-converted light-emitting diodes (pc-LEDs). Large micro-size cube phosphors (~100 μm) are newly designed and prepared as scatter-free phosphors, combining the two scatter-free conditions of particles based on Mie's scattering theory; the grain size or grain boundary was smaller than 50 nm and the particle size was larger than 30 μm . A careful evaluation of the conversion efficiency and packaging efficiency of the large micro-size cube phosphor-based white pc-LED demonstrated that large micro-size cube phosphors are an outstanding potential candidate for scatter-free phosphors in white pc-LEDs. The luminous efficacy and packaging efficiency of the $\text{Y}_3\text{Al}_5\text{O}_{12}:\text{Ce}^{3+}$ large micro-size cube phosphor-based pc-LEDs were 123.0 lm/W and 0.87 at 4300 K under 300 mA, which are 17% and 34% higher than those of commercial powder phosphor-based white LEDs (104.8 lm/W and 0.65), respectively. In addition, the introduction of large micro-size cube phosphors can reduce the wide variation in optical properties as a function of both the ambient temperature and applied current compared with those of conventional powder phosphor-based white LEDs.

© 2012 Optical Society of America

OCIS codes: (220.0220) Optical design and fabrication; (230.3670) Light-emitting diodes; (290.0290) Scattering; (290.4020) Mie theory.

References and links

1. S. Nakamura, T. Mukai, and M. Senoh, "Candela-class high-brightness InGaN/AlGaIn double-heterostructure blue-light-emitting diodes," *Appl. Phys. Lett.* **64**(13), 1687–1689 (1994).
2. S. Nakamura, M. Senoh, N. Iwasa, S. Nagahama, T. Yamada, and T. Mukai, "Superbright green InGaIn single-quantum-well-structure light-emitting diodes," *Jpn. J. Appl. Phys.* **34**(Part 2, No. 10B), L1332–L1335 (1995).
3. S. Nakamura, M. Senoh, N. Iwasa, and S. Nagahama, "High-power InGaIn single-quantum-well-structure blue and violet light-emitting diodes," *Appl. Phys. Lett.* **67**(13), 1868–1870 (1995).
4. P. Schlotter, R. Schmidt, and J. Schneider, "Luminescence conversion of blue light emitting diodes," *Appl. Phys., A Mater. Sci. Process.* **64**(4), 417–418 (1997).
5. P. F. Smet, A. B. Parmentier, and D. Poelman, "Selecting conversion phosphors for white light-emitting diodes," *J. Electrochem. Soc.* **158**(6), R37–R54 (2011).
6. V. Bachmann, C. Ronda, and A. Meijerink, "Temperature quenching of yellow Ce^{3+} luminescence in YAG:Ce," *Chem. Mater.* **21**(10), 2077–2084 (2009).
7. N. Narendran, Y. Gu, J. P. Freyssonier-Nova, and Y. Zhu, "Extracting phosphor-scattered photons to improve white LED efficiency," *Phys. Status Solidi A* **202**(6), R60–R62 (2005).
8. K. Yamada, Y. Imai, and K. Ishii, "Optical simulation of light source devices composed of blue LEDs and YAG phosphor," *J. Light Vis. Environ.* **27**(2), 70–74 (2003).
9. L. Wang, L. Mei, G. He, J. Li, and L. Xu, "Preparation of Ce:YAG glass-ceramics with low SiO_2 ," *J. Am. Ceram. Soc.* **94**(11), 3800–3803 (2011).
10. S. Fujita, A. Sakamoto, and S. Tanabe, "Luminescence characteristics of YAG glass-ceramic phosphor for white LED," *IEEE J. Sel. Top. Quantum Electron.* **14**(5), 1387–1391 (2008).
11. S. Fujita, S. Yoshihara, A. Sakamoto, S. Yamamoto, and S. Tanabe, "YAG glass-ceramic phosphors for white LED (I): development," *Proc. SPIE* **5941**, 594111, 594111-7 (2005).
12. S. Nishiura, S. Tanabe, K. Fujioka, and Y. Fujimoto, "Properties of transparent Ce:YAG ceramic phosphors for white LED," *Opt. Mater.* **33**(5), 688–691 (2011).
13. H. K. Park, J. R. Oh, and Y. R. Do, "2D SiN_x photonic crystal coated $\text{Y}_3\text{Al}_5\text{O}_{12}:\text{Ce}^{3+}$ ceramic plate phosphor for high-power white light-emitting diodes," *Opt. Express* **19**(25), 25593–25601 (2011).

14. J. W. Kim and Y. J. Kim, "The effects of substrates and deposition parameters on the growing and luminescent properties of $Y_3Al_5O_{12}:Ce$ thin films," *Opt. Mater.* **28**(6-7), 698–702 (2006).
15. W.-H. Chao, R.-J. Wu, and T.-B. Wu, "Structural and luminescent properties of YAG:Ce thin film phosphor," *J. Alloy. Comp.* **506**(1), 98–102 (2010).
16. J. Ryszkowska, "Quantitative description of the microstructure of polyurethane nanocomposites with YAG including Tb^{3+} ," *Mater. Sci. Eng. B* **146**(1-3), 54–58 (2008).
17. M. Nyman, L. E. Shea-Rohwer, J. E. Martin, and P. Provencio, "Nano-YAG:Ce mechanisms of growth and epoxy-encapsulation," *Chem. Mater.* **21**(8), 1536–1542 (2009).
18. R. Kasuya, A. Kawano, T. Isobe, H. Kuma, and J. Katano, "Characteristic optical properties of transparent color conversion film prepared from YAG:Ce³⁺ nanoparticles," *Appl. Phys. Lett.* **91**, 111916 (2007).
19. B. K. Park, H. K. Park, J. H. Oh, J. R. Oh, and Y. R. Do, "Selecting morphology of $Y_3Al_5O_{12}:Ce^{3+}$ phosphors for minimizing scattering loss in the pc-LED package," *J. Electrochem. Soc.* **159**(4), J96–J106 (2012).
20. Y. X. Pan, W. Wang, G. K. Liu, S. Skanthakumar, R. A. Rosenberg, X. Z. Guo, and K. K. Li, "Correlation between structure variation and luminescence red shift in YAG:Ce," *J. Alloy. Comp.* **488**(2), 638–642 (2009).
21. H. Yang, D.-K. Lee, and Y.-S. Kim, "Spectral variations of nano-sized $Y_3Al_5O_{12}:Ce$ phosphors via codoping/substitution and their white LED characteristics," *Mater. Chem. Phys.* **114**(2-3), 665–669 (2009).
22. S. Fujita, Y. Umayahara, and S. Tanabe, "Influence of light scattering on luminous efficacy in Ce:YAG glass-ceramic phosphor," *J. Ceram. Soc. Jpn.* **118**(2), 128–131 (2010).
23. J. Lu, K. Ueda, H. Yagi, T. Yanagitani, Y. Akiyama, and A. A. Kaminskii, "Neodymium doped yttrium aluminum garnet ($Y_3Al_5O_{12}$) nanocrystalline ceramics—a new generation of solid state laser and optical materials," *J. Alloy. Comp.* **341**(1-2), 220–225 (2002).
24. T. Yanagida, H. Takahashi, T. Ito, D. Kasama, T. Enoto, M. Sato, S. Hirakuri, M. Kokubun, K. Makishima, T. Yanagitani, H. Yagi, T. Shigeta, and T. Ito, "Evaluation of properties of YAG (Ce) ceramic scintillators," *IEEE Trans. Nucl. Sci.* **52**(5), 1836–1841 (2005).
25. J. H. Oh, J. R. Oh, H. K. Park, Y.-G. Sung, and Y. R. Do, "Highly-efficient, tunable green, phosphor-converted LEDs using a long-pass dichroic filter and a series of orthosilicate phosphors for tri-color white LEDs," *Opt. Express* **20**(S1), A1–A12 (2012).

1. Introduction

White light phosphor-converted light-emitting diodes (pc-LEDs) are obtained via a combination of the transmission of the blue emission through phosphors from blue InGaN LEDs and the broad yellow emission from $Y_3Al_5O_{12}:Ce^{3+}$ (YAG:Ce) phosphors because the blue and yellow emissions are complementary colors [1–4]. The YAG:Ce phosphor-based white pc-LEDs comprise a significant portion of the LED white lighting market due to their broad emission spectrum, high absorption strength, excellent thermal quenching, high quantum efficiency, excellent chemical stability, and fast decay time. Although the internal quantum efficiency (IQE) of the YAG:Ce micro-size powder phosphor (MPP) is over 0.9 [5, 6], considerable effort has been made to develop highly efficient YAG:Ce-based white pc-LEDs for applications in solid state lighting, because micro-size powder-based pc-LEDs provide limited conversion efficiency (CE) for emission from the powder phosphor layer. This low CE (~0.62 at a YAG:Ce MPP concentration of 25 wt% in paste) is due to the high scattering and reflecting loss of the blue excitation and yellow emission light from the coated micro-size phosphor particles [7, 8].

In an effort to address the high scattering/reflection loss of micro-size phosphors, new types of white LEDs incorporating YAG:Ce glass ceramic phosphors (GCPs) [9–11], transparent polycrystalline YAG:Ce ceramic plate phosphors (CPPs) [12, 13], thin-film phosphors (TFPs) [14, 15], or YAG:Ce nanophosphors (NPs) in transparent matrix [16–18] have been suggested recently by many research groups, including our group. Although the development of highly efficient pc-LEDs with scatter-free phosphors has been undertaken by various research groups, significant progress has not yet been made in replacing the commercialized MPPs due to the problems encountered during the new scatter-free phosphor implementation. The transparent film-type phosphors, which were intentionally developed in order to minimize the scattering/reflection loss of MPPs, have suffered from limited extraction efficiency and limited fabrication nature of assembly with a blue LED package [19]. Therefore, it is necessary to develop a new morphologically modified YAG:Ce phosphor that can satisfy the requirements for scatter-free phosphors and be easily implemented in a pc-LED package, so that they can replace MPPs in conventional white pc-LEDs.

Based on Mie's scattering theory, phosphors must satisfy two morphological conditions in order to be considered good candidates for scatter-free phosphors. Firstly, if the particle size

of the phosphor is smaller than 50 nm, and the NP-based matrix composite is transparent in the visible range based on Mie's scattering theory [20, 21], scattering loss can be neglected in the NP film as shown in the relationship between the scattering coefficient and the nanoscale size of particles in the inset of Fig. 1. Secondly, the luminous efficacy of film-type phosphors is increased with an increase in the particle sizes of transparent film-type polycrystalline phosphors while the light scattering coefficient is decreased. The increase in luminous efficacy is attributed to the decreasing light scattering coefficient with increases in the particle size as large as possible over $\sim 30 \mu\text{m}$ [22], as shown in Fig. 1. Therefore, if the newly modified phosphors simultaneously have a small grain size or grain boundary ($< 50 \text{ nm}$) inside the crystal and a large phosphor particle size ($> 30 \mu\text{m}$), the phosphors can lead to an overall smaller scattering loss compared with the conventional micro-size YAG:Ce in polymer or silicone.

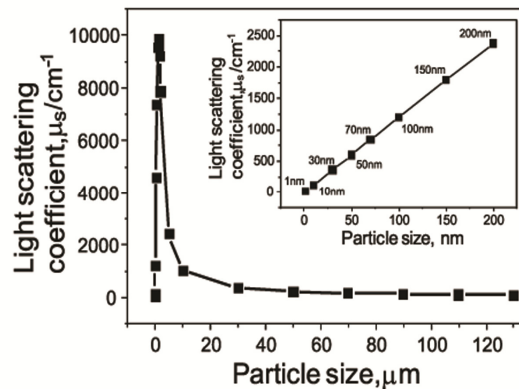


Fig. 1. Calculated light scattering coefficient, μ_s , with YAG:Ce particle size. Inset shows calculated light scattering coefficient with nanoscale size of YAG:Ce particles.

In this paper, transparent YAG:Ce large micro-cube phosphors with diameters of $\sim 100 \mu\text{m}$ and grain boundary width of $\sim 1 \text{ nm}$ are designed and prepared in order to enhance the CE and the packaging efficiency (PE) of white pc-LEDs implemented with large micro-size cube phosphor paste. In addition, YAG:Ce large micro-cube phosphors are introduced in order to demonstrate the method of satisfying the boundary conditions required for scatter-free phosphors; this can also lead to further research and development technologies related to morphologically new phosphors that can satisfy the required boundary conditions. The approach toward the creation of new large micro-cube phosphors as demonstrated in this work has greater potential for minimizing scattering loss, enhancing the CE and PE of white pc-LEDs during implementation, and providing efficient phosphor capabilities beyond conventional micro-size powder-based white pc-LEDs.

2. Experimental methods

YAG:Ce CPPs $100 \mu\text{m}$ thick were purchased from Balkowski Japan Co. Ltd. The preparation of the YAG:Ce CPP was similar to that described in previous publications [23, 24], where an average grain size of about $> 10 \mu\text{m}$, a pore volume of about 1 ppm and a grain boundary width of about 1 nm were reported. Large micro-size cube phosphors ($100 \times 100 \times 100 \mu\text{m}$) could be fabricated by dicing a $100\text{-}\mu\text{m}$ thick CPP into $100 \mu\text{m}$ squares using a diamond wheel. Figure 2 shows schematic diagram of the fabrication process of the YAG:Ce large micro-size cube phosphors. KER-2500A and B (Shin-Etsu Chemical Co. Ltd.) were used as the silicone binder resin (paste) for the encapsulation of the LEDs. KER-2500A and B were mixed at a weight ratio of 1:1 and were then mixed with phosphor as a function of the phosphor concentration (wt%) in the silicone binder. After mixing, the mixture was inserted into the LED cup and was then cured at $150 \text{ }^\circ\text{C}$ for 1 hour. Commercial YAG:Ce powders (LP-6979) were obtained from LWB Corp.

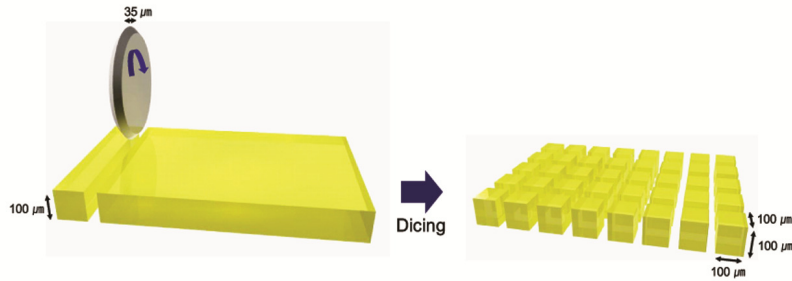


Fig. 2. Schematic diagram of the fabrication process of the YAG:Ce large micro-size cube phosphors.

To measure the light scattering coefficients of both the conventional powder phosphor and large micro-size cube phosphors as a function of the phosphor concentration, both phosphors (10 (powder: 2.5 vol%, cube: 2.4 vol%), 20 (5.5, 5.2 vol%), 30 (9, 8.5 vol%), 40 (13.3, 12.7 vol%), and 50 wt% (18.8, 17.9 vol%)) dispersed in silicone binder (paste) were screen-printed on glass substrates to a thickness of 200 μm and were then cured at 150 $^{\circ}\text{C}$ for 1 hour.

To fabricate the newly developed micro-size cube-based white pc-LEDs, large micro-size cube phosphors (5 (1.1 vol%), 10 (2.4), 20 (5.2), 30 (8.5), 40 (12.7), 45 (15.1), 50 (17.9), and 55 wt% (21)) dispersed in silicone binder (paste) were directly coated onto a blue InGaN LED chip as a function of the phosphor concentration in the silicone binder. For a comparison of a conventional powder phosphor and the large micro-size cube phosphors, conventional micro-size powder-based white LEDs (5 (1.2 vol%), 10 (2.5), 15 (3.9), 20 (5.5), 25 (7.1), 30 (9), 40 (13.3), 50 (18.8), and 60 wt% (25.7)) were fabricated using the same method.

A low-magnification surface image of the YAG:Ce large micro-cube phosphors was obtained by a field-emission typed scanning electron microscopy (FE-SEM) (JSM 7401F, JEOL) operated at 10 kV. A top-view fluorescent image of the YAG:Ce large micro-cube phosphors was taken using a fluorescence microscope (IX71, Olympus). The surface morphology of the YAG:Ce large micro-cube phosphors was measured by atomic force microscopy (AFM) (Seiko Instruments, model SPA 400) operated in contact mode (Si cantilever). The crystal structure of the YAG:Ce large micro-cube phosphors was measured by X-ray diffraction (XRD, X'pert system, Philips) with $\text{Cu K}\alpha_1$ radiation over a range of 10° - 80° 2θ at a scan rate of 1° $2\theta/\text{min}$. The optical transmittance of the YAG:Ce CPP was measured over the wavelength region of 380 to 1100 nm using a UV/Vis spectrophotometer (OPTIZEN 2120UV, MECASYS). The transmittances of the powder phosphor/silicone binder and cube phosphor/silicone binder mixed thick films with a 50 wt% concentration in the silicone binder were measured using white light in the wavelength region of 550 to 750 nm. In addition, The transmittances of the yellow light (about 557nm) for the powder phosphor/silicone binder and cube phosphor/silicone binder mixed thick films as a function of the phosphor concentration in the silicone binder were measured using yellow light (about 557nm) in the normal mode. The electroluminescent (EL) properties of two pc-LEDs implemented with the conventional YAG:Ce micro-size phosphors and the large micro-cube phosphors were measured under 450nm LED excitation using a spectrophotometer (PSI Co. Ltd. Model Darsa II) with integrated spheres as a function of the phosphor concentration in a phosphor binder paste, under applied current and at ambient temperatures. As described in a previous publication [5], the internal quantum efficiency (IQE) of the large micro-size cube phosphor (~ 0.82) was obtained by comparing the integrated emission intensity and the integrated absorption intensity of YAG cube phosphors with the well-established IQE (~ 0.95) of conventional YAG:Ce powder phosphors (LP-6979). The conversion efficiency (CE) of a phosphor in a pc-LED should also be considered when assessing a specific phosphors incorporated into a pc-LED device. The CE of a pc-LED depends on two main factors: the IQE of the phosphor and the packaging efficiency (PE) of the LED [5, 25]. The CE is the ratio between the number of emitted photons and the number of incident photons in the pc-LED

package. In other words, this equals the IQE times the PE. The PE is defined as the ratio of the extracted emission light from the LED package to the emitted light from the phosphors within the pc-LED package.

3. Results and discussion

The large micro-size cube phosphors were prepared by dicing a 100 μm thick CPP into 100 μm squares using a diamond wheel. Figures 3(a) and 3(b) show a low magnification, top view FE-SEM image and a top view fluorescence microscope image of a YAG:Ce large micro-cube phosphor. These figures indicate that $\sim 100 \mu\text{m}$ YAG:Ce cubes with precise edges were obtained as designed prior to cutting the cubes. The top view two dimensional AFM image shown in Fig. 3(c) indicates that the root-mean-square (RMS) roughness was approximately $\sim 0.42 \text{ nm}$ and the grains had boundaries that were not easily distinguishable. Both the particle size ($\sim 100 \mu\text{m}$) of the cube and the grain boundary width ($\sim 1 \text{ nm}$) inside the cube appeared to satisfy the requirements for the scatter-free phosphors as mentioned above.

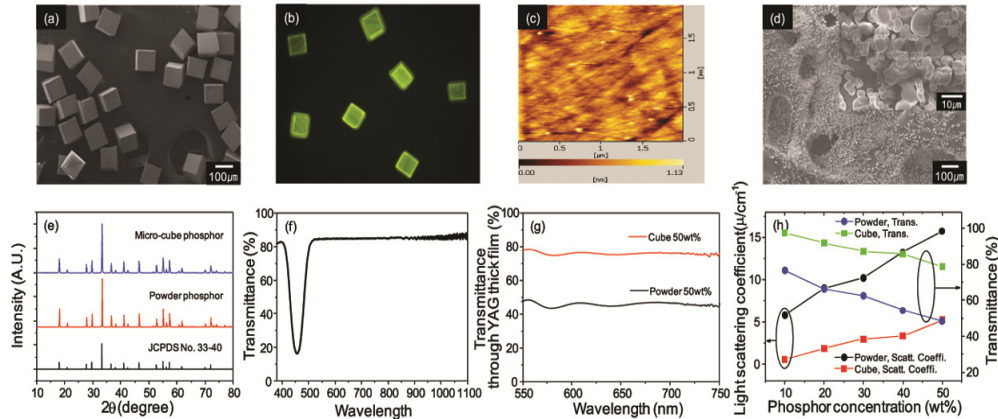


Fig. 3. (a) Low magnification, top view FE-SEM image, (b) Top view fluorescent image, and (c) Two dimensional AFM image of YAG:Ce large micro-size cube phosphors. (d) Low- and high-magnification FE-SEM images of conventional YAG:Ce micro-size powder phosphors. (e) XRD patterns of YAG:Ce powder phosphors and large micro-size cube phosphors. (f) Optical transmittance spectra of a YAG:Ce ceramic plate phosphor. (g) Transmittance spectra of white light (in the wavelength region of 550 to 750nm) through YAG:Ce powder phosphor and large micro-size cube phosphor thick film (h) Measured light scattering coefficients and transmittance at yellow light (about 557nm) of both a conventional powder phosphors and a large micro-size cube phosphors as function of the phosphor concentration in the paste.

Figure 3(d) shows low- and high-magnification FE-SEM images of conventional YAG:Ce MPPs. These figures indicate that the size of the conventional YAG:Ce MPPs ($\sim 10 \mu\text{m}$) is much smaller than that of cube phosphors. The nature of the large micro-size cube phosphors is equal to that of ceramic plate phosphors excepting the morphological appearance. Figure 3(e) indicates that the observed XRD patterns of the conventional YAG:Ce MPPs and the large micro-cube YAG:Ce phosphors were well matched to the lines of the YAG phase specified in the JCPDS files (No. 33-0040). The optical transmittance of the YAG:Ce CPP of $\sim 80\%$ at 550 nm, as shown in Fig. 3(f), confirms that the YAG:Ce large micro-size cube phosphors are optically transparent in the visible wavelength range [13]. Furthermore, a comparison of the light scattering coefficient between conventional MPPs and large micro-size cube phosphors provided clear evidence of the capability of reducing light scattering by each phosphor. Based on Lambert-Beer's law, the light scattering coefficient, μ , is as follows [22]:

$$\mu = -\frac{\log T}{d} \quad (1)$$

where T is the transmittance and d is the thickness of the YAG:Ce phosphor/silicone binder mixed film. The transmittance data of white light (in the wavelength region of 550 to 750nm) through the YAG:Ce thick film, which is composed of a silicone binder (paste) and a YAG:Ce phosphor with 50 wt% concentration in the silicone binder such as the conventional MPPs and the large micro-cube phosphors, indicate that the cube phosphors have higher transparency than the MPPs, as shown in Fig. 3(g). Figure 3(h) shows the measured scattering coefficients and the transmittance of the yellow light (about 557nm) of both the conventional powder phosphors and large micro-size cube phosphors as function of the phosphor concentration in the paste. The measured scattering coefficients of both phosphors increased as the phosphor concentration in the paste increased, while the transmittance of yellow light (557nm) decreased. The figure clearly demonstrates that the scattering coefficient of the newly developed large micro-cube phosphors was significantly decreased compared with that of conventional MPPs. The figure also shows that the transmittance of yellow light by the large micro-cube phosphors showed a significant increase compared to the use of conventional MPPs. Therefore, large micro-size cube phosphors demonstrated reduced light scattering and increased transparency in the visible wavelength range and provided clear evidence for minimizing the scattering loss of phosphors in the pc-LED package.

Schematic diagrams of the conventional powder phosphor-based and the large micro-size cube-based LED device structure are shown in Figs. 4(a) and 4(b). For the fabrication of both LEDs, the conventional phosphors and diced large micro-size cube phosphors were dispersed in silicone binder (paste) and were then directly coated onto a blue InGaN LED chip. In order to observe the scatter-free capability of the newly developed YAG:Ce large micro-cube phosphors, the luminous efficacy, CE, and PE of two pc-LEDs implemented with the conventional micro-size phosphors and the large micro-cube phosphors were compared as a function of phosphor concentration in a phosphor binder paste as shown in Figs. 4(c) to 4(f). Figure 4(c) shows the luminous efficacy (lm/W) of both the micro-size powder phosphors and the large micro-size cube phosphors as a function of the phosphor concentration in the paste. The luminous efficacy of the conventional micro-size phosphors reached a maximum point at a relatively low phosphor concentration (15 wt%) in the paste and then decreased slowly after saturation. As the phosphor concentration increased, the particle number density of the phosphor layer became higher. Accordingly, the blue light was significantly blocked, scattered, and absorbed at the phosphor layer, and a large portion of yellow light was also scattered and wasted. However, the luminous efficacy of the large micro-cube phosphors increased with the increase of the phosphor concentration in the cube phosphors in the paste and reached a maximum point at a relatively high concentration (50 wt%) of micro-cube phosphors. Then, the luminous efficacy decreases slowly with increases in the phosphor concentration after the maximum point. The maximum luminous efficiency of the large micro-size cube phosphor-based pc-LEDs was 123.0 lm/W at a phosphor concentration of 50 wt%, which is ~11% higher than that of conventional powder phosphor-based white LEDs (111.0 lm/W at a phosphor concentration of 15 wt%). The maximum luminous efficacy obtained at a high phosphor concentration suggests that the micro-cube phosphors show reduced scattering loss due to the large-size cubes with small grain boundaries.

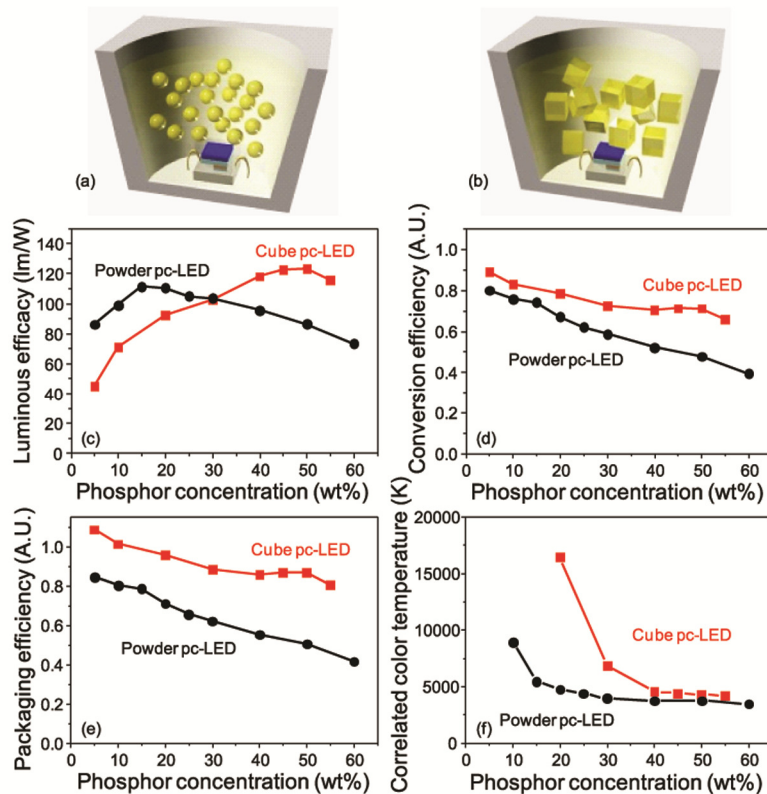


Fig. 4. Schematic diagrams of (a) a YAG:Ce conventional powder phosphor-based and (b) a large micro-size cube-based LED device structure. (c) Luminous efficacy (lm/W), (d) Conversion efficiency, (e) Packaging efficiency, and (f) Correlated color temperature (CCT) of both a conventional powder-based and a large micro-size cube-based LED as a function of the phosphor concentration in the paste.

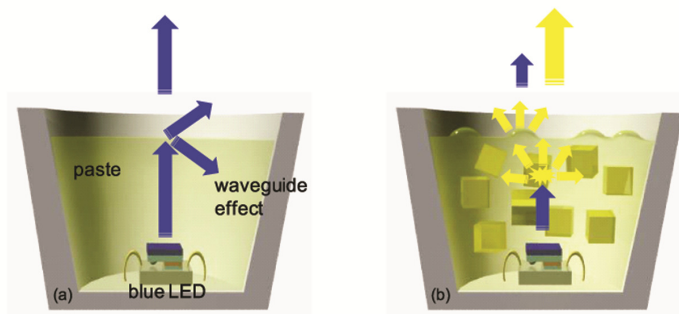


Fig. 5. Schematic diagrams of the light paths within silicone binder (paste) in LED package (a) without and (b) with the large micro-size cube phosphors.

Figures 4(d) and 4(e) show the CE and PE of both the conventional micro-size powder phosphors and the large micro-size cube phosphors as a function of phosphor concentration in the paste. The PE gap between the YAG:Ce micro-cube phosphors and conventional powder phosphors was enlarged compared with the CE gap between them. This is a result of the internal quantum efficiency (IQE) of the conventional powder phosphors (~ 0.95) being higher than that of the large micro-cube phosphors (~ 0.82) and the PE factor of the large micro-size cube phosphors being enhanced. The PE of the conventional powder phosphor-based LED

and large micro-size cube phosphor-based LED decreased from 0.84 to 0.50 and from 1.08 to 0.87, respectively, with the increase in the phosphor concentration from 5 to 50 wt%. Figures 5(a) and 5(b) show schematic diagrams of the light paths within the silicone binder (paste) in the LED package without and with the large micro-size cube phosphors. As shown in Fig. 5(a), among the blue light emitted from LED chip, only light emitted at an angle of less than the critical angle can escape. All other light trapped within the paste with a flat surface is wave-guided. This indicates that a non-negligible portion of the blue light emitted from the LED chip remains and circulates in the LED package due to the total internal reflection (TIR) and waveguide effect. In contrast, when transparent micro-size phosphors exist inside the paste of a LED chip and when the surface of the paste has a corrugated structure caused by the phosphors, a large portion of the blue light confined inside the paste can be used as excitation light for the phosphors. The emitted yellow light can then be perturbed outwards paste, as shown in Fig. 5(b). This is due to the combined effect of the change in the path of the newly emitted yellow light by the transparent micro-size phosphors and the surface scattering created by the corrugated structure of the paste. Thus, due to the increased amount of yellow light converted by blue light in a pc-LED implemented with transparent micro-size phosphors, the PE of white pc-LED can become higher than 1.0 at the low concentration range of cube phosphors. Thus, the PE of the large micro-size cube phosphor-based LED became higher (1.08) than 1.0 via the aforementioned phenomenon. The enhancement ratio of PE according to the large micro-size cube phosphor increased from 1.29 to 1.74 fold with an increase of the phosphor concentration from 5 to 50 wt% in the paste. This result confirms that the reduced scattering loss of the large micro-cube phosphors is increasingly important at higher phosphor concentrations.

Figure 4(f) also shows the correlated color temperature (CCT) of both the conventional powder phosphor-based and the large micro-size cube-based LED as a function of the phosphor concentration in order to verify the same white light (4300 K) for both systems. Figures 4(c) and 4(f) indicate that the phosphor concentrations required to obtain a CCT of ~4300 K for the conventional powder-based and large micro-size cube-based LEDs were 25 wt% and 50 wt%, respectively. At 4300 K, the luminous efficacy of the large micro-cube phosphor-based LED was 123.0 lm/W at 300 mA (rated current), which is higher than that of the conventional powder phosphor-based white LEDs (104.8 lm/W).

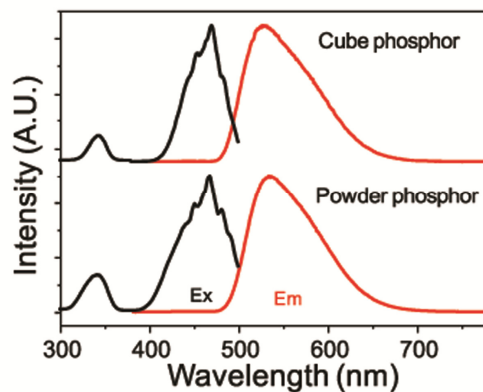


Fig. 6. Excitation and emission spectra of a YAG:Ce conventional powder phosphor and a large micro-size cube phosphor.

Figure 6 shows the excitation and emission spectra of a YAG:Ce conventional powder phosphor and a large micro-size cube phosphor. The excitation and emission peaks of the large micro-size cube phosphor show similar features compared to those of the conventional powder phosphor. This indicates that the conventional powder phosphor and the cube phosphor have similar chemical compositions. Figure 7(a) shows the electroluminescent (EL) emission spectra of the conventional powder-based (25 wt%) LED and the micro-size cube-

based (50 wt%) LED at 4300 K in an equal-current condition (300 mA). The same shapes of the transmitted blue peaks and emitted yellow peaks in the EL spectra between the powder-based LED and the cube-based LED result from the similar excitation and emission peaks caused by the similar chemical compositions of the YAG:Ce powder phosphor and the cube phosphor. Thus, it can be concluded that the considerable enhancement (~17%) of the luminous efficacy and the increased intensity of the yellow emission caused by the large micro-cube phosphor-based LED are primarily due to the effect of the enhancement of the packaging efficiency (~34%), although the IQE value of the cube phosphors is lower than that of conventional powder phosphors.

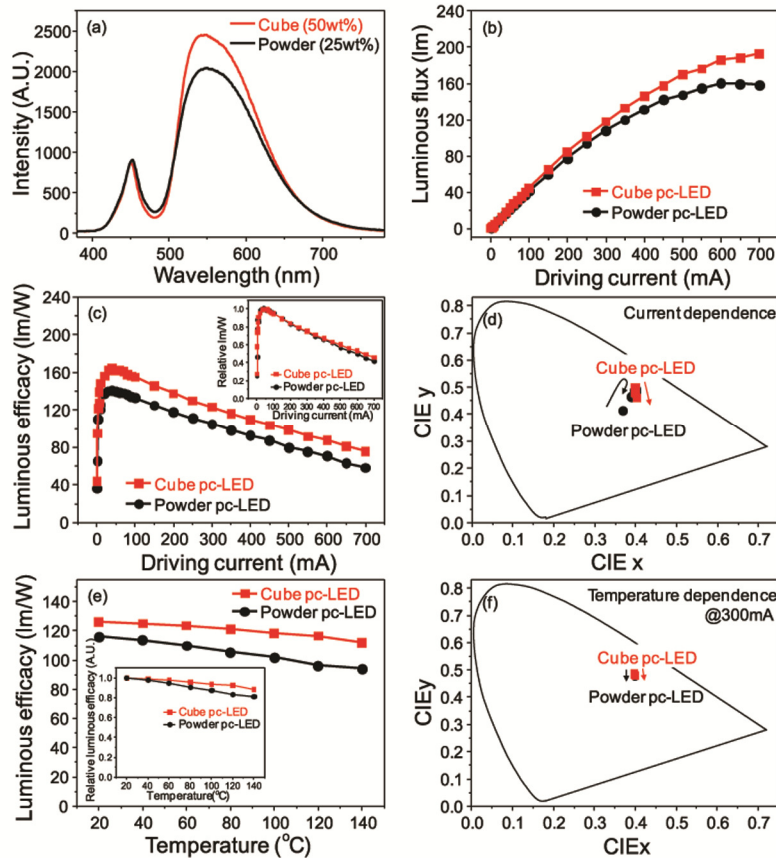


Fig. 7. (a) Blue-conversion-white electroluminescent (EL) emission spectra of a conventional powder-based (with powder concentration of 25 wt%) and a large micro-size cube-based (with powder concentration of 50 wt%) LED at 4300K in an equal-current condition (300 mA). (b) Luminous flux (lm), (c), (e) Luminous efficacies (lm/W) and (d), (f) Color coordinates of the conventional powder phosphor-based (with powder concentration of 25 wt%) and the large micro-size cube-based LED (with powder concentration of 50 wt%) as a function of the applied current and the ambient temperature. Insets in (c), (e) show relative luminous efficacies of the conventional powder-based (25 wt%) and the large micro-size cube-based LED (50 wt%) as a function of the applied current and the ambient temperature.

In addition, the detailed EL properties were compared as functions of both the applied current and ambient temperature in order to analyze the suitability of the YAG:Ce large micro-size cube phosphors for application in high power LEDs. Plots of the luminous flux (lm), luminous efficacy (lm/W) and color coordinates for conventional MPP-based and micro-cube phosphor-based LEDs as a function of the applied current are shown in Figs. 7(b) to 7(d). The luminous flux of the conventional powder-based LED was lower than that of the

large micro-size cube-based LED with an increase in the applied current from 1 to 700 mA, as shown in Fig. 7(b). In addition, Fig. 7(c) shows that the luminous efficacy of the conventional powder-based and large micro-size cube-based LED decreased from 140.8 lm/W to 57.9 lm/W and from 164.5 lm/W to 75.3 lm/W, respectively, with an increase in the applied current from 40 to 700 mA. The enhancement ratio of the luminous efficacy according to the large micro-cube phosphor was increased from 1.17 to 1.30 with the increase of the applied current. The relative luminous efficacy shown in the inset of Fig. 7(c) indicates that the decrease in the luminous efficacy of the conventional powder-based LED is slightly faster than that of the large micro-size cube-based LED with an increase in the applied current from 1 to 700 mA. The decreased trend of both LED types with an increase in the current was caused by the combined effects of the current degradation of the blue LED chip and the thermal degradation of the conventional powder and micro-cube phosphors with an increase in the current. This is because both the conventional powder phosphors and large micro-cube phosphors are in direct contact with the blue LED chip in both the conventional powder-based and cube-based white pc-LED. Figure 7(d) shows that the variation of the color coordinates for the conventional powder-based LED is larger than that for the large micro-size cube-based LED with an increase in the applied current from 1 to 700 mA. This also indicates that the introduction of the large micro-cube phosphors in the white pc-LED improves the current stabilities of the color coordinates. Thus, it can be speculated that the improved current dependence of the large micro-cube phosphor-based LED is only due to the slower thermal quenching behavior of the micro-cube phosphors compared with the conventional powder phosphors.

Figures 7(e) and 7(f) compare the efficacy and color coordinate stability at the same current (300 mA) with an increase in the ambient temperature. Figures 7(e) indicates that the introduction of the large micro-cube phosphors in the white pc-LED improves the temperature stabilities of the efficacies. Figure 7(f) shows that the variation of the color coordinates for the conventional powder-based LED and large micro-size cube-based LED is similar and that both LEDs are stable at typical LED temperatures. These outcomes are due to the minimized scattering loss from the large micro-size YAG:Ce cube phosphors, which can reduce thermal loss. For these reasons, the fast degradation of the conventional powder-based white LED is caused by the complex effects of both the current/thermal degradation of the blue LED and the thermal quenching of the powder phosphors. Therefore, the improved current and temperature stabilities confirm the suitability of the large micro-cube YAG:Ce phosphors for use in high power white LEDs.

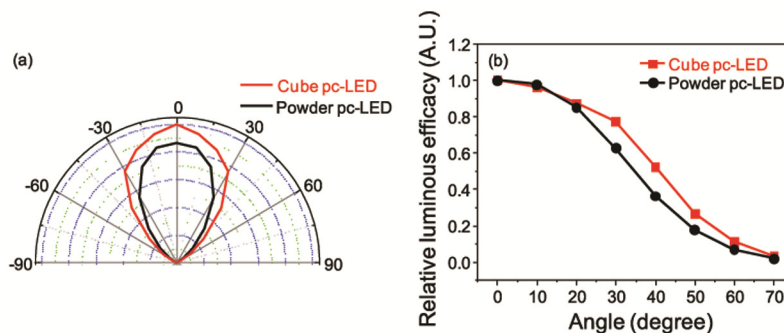


Fig. 8. (a) The relative lumens and (b) normalized luminous efficacy as a function of the viewing angle for a conventional powder-based LED and a large micro-size cube-based LED taken under identical excitation conditions (current at 300 mA).

The angular dependence of the emission spectrum was also examined to compare the difference between the conventional powder-based LED and the large micro-size cube-based LED in terms of the viewing angle. Figure 8 plots the measured relative lumens and normalized luminous efficacy as a function of the viewing angle for two different LEDs taken

under identical excitation conditions (current at 300 mA). The figure shows that the emission of the cube-based LED is stronger than that of the conventional powder-based LED at all viewing angles. The luminous efficacies of both LEDs show similar Lambertian behaviors. Hence, the proposed cube-based pc-LED clearly shows variation comparable to that of a powder-based pc-LED in terms of its angular radiation patterns over a large angular span.

4. Conclusions

This study evaluated the influence of light scattering on the luminous efficacy, conversion efficiency, and packaging efficiency of pc-LEDs using conventional micro-size powder phosphors and the newly developed large micro-size cube phosphors. The increased luminous efficacy, conversion efficiency, and packaging efficiency of the newly developed large micro-size cube phosphors were primarily attributed to the decrease in the light scattering loss due to the reduced light scattering coefficient in the visible light through satisfying the scatter-free conditions of phosphor morphology as mentioned above. Therefore, the method for decreasing the light scattering from phosphor-converted LEDs should be an important design parameter of phosphor morphologies in order to maximize the packaging efficiency of white pc-LED packages. These requirements for scatter-free phosphors are expected to be morphologically important criteria in the design and synthesis of new inorganic phosphors in white pc-LED applications.

Acknowledgments

This work was supported by the National Research Foundation (NRF) grant (no. 2011-0017449) funded by the Ministry of Education, Science and Technology (MEST) of Korea.